KYODO YUSHI TECHNICAL BULLETIN

No.1 January 1, 2014

GREASE FORMS THICK ELASTOHYDRODYNAMIC LUBRICATION FILM AT LOW SPEEDS

Many rolling contacts in practical applications are lubricated with grease, where the ease of application has been considered to be its main reason. However, it has been found that grease forms thicker elastohydrodynamic(EHL) film than lubricating oil at low speeds, which must has contributed to lower friction torques at low speeds and to prevention of surface damage like fretting.

Film thickness of grease was determined in rolling contact between a glass disk and a steel ball of 19.05mm in diameter in pure rolling contact under a load of 20N at room temperature by ultrathin-film optical interferometry "SLIM" developed in Imperial College, Fig.1.

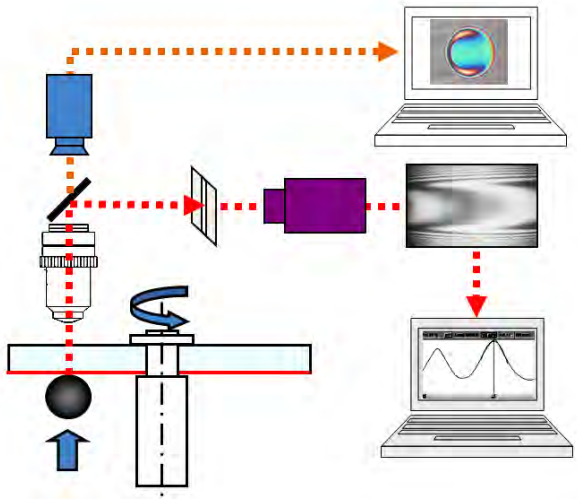

Fig.1 Interferometry setup

Three sample greases A, B, C were prepared with synthetic hydrocarbon of different viscosity, A:25mm^2/s, B:81mm^2/s, C:741mm^2/s, as the base oils and lithium stearate as the thickener; the concentration of the thickener was adjusted to have a consistency number 3.

The measured central film thickness with grease A:▲, B:■, C:● is plotted against entrainment speed in Fig.2, where the three lines show the central film thickness with their base oils alone. At higher speeds, the greases formed films thicker than their base oils alone but followed the EHL theory. On decreasing speeds, however, the film thickness of grease deviates from the EHL theory. After taking a minimum it increases again with the further decrease in the speed to form much thicker film than their base oil.

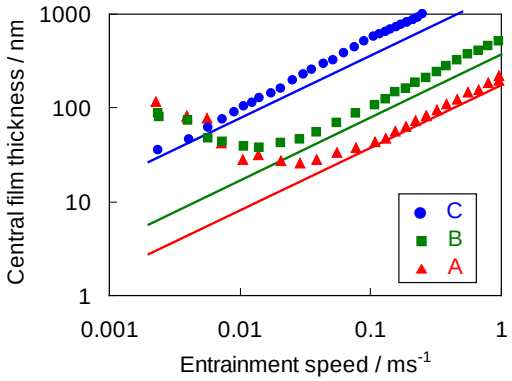

Fig.2 Change in central film thickness with speed

Different grease causes diferent extent of increase in the film thickness at low speed. Figure 2 shows its difference caused by different base oil viscosity, but it is also caused by the different type of the thickener.

The nature of the thick films at low speeds has been under discussion and it could differ depending on the conditions as well as greases. In the present case, interferometry revealed that, although thin, the "horseshoe" peculiar to EHL film was clearly observed at very low speed as is shown in Fig.3.

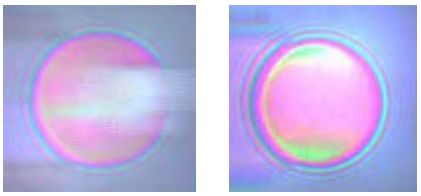

0.004ms^{-1} 0.22ms^{-1}

Fig.3 "Horseshoe" with grease A

Y. Kimura, T. Endo and D. Dong, "EHL with grease at low speeds", Jianbin Luo, Yonggang Meng, Tianmin Shao and Qian Zhao (eds.), Advanced Tribology - Proceedings of CIST2008 & ITS-IFToMM2008 Beijing, China (2009) pp.15-19.

KYODO YUSHI TECHNICAL BULLETIN

No.2 January 1, 2014

WHY GREASE FORMS THICK ELASTOHYDRODYNAMIC LUBRICATION FILM AT LOW SPEEDS? — A SIMPLIFIED ANALYSIS

Analysis has been made of the mechanism of forming thick elastohydrodynamic(EHL) film of grease by using "Carreau-Yasuda equation", which depicts a transition of a generalized viscosity from high Newtonian viscosity at low shear rates to low Newtonian viscosity at high shear rates. It has been concluded that, while thick EHL film is formed by high entrainment rates at high speed, increased viscosity at low shear rates causes it at low speeds.

To express non-Newtonian viscosity of grease, a generalized viscosity η^* is introduced, which is defined by the ratio of the amplitudes of the shear stress and the shear strain when grease is sheared in an oscillation manner.

$$\eta^* = (\mu_1-\mu_2)\{1+(\lambda\dot{\gamma})^a\}^{(n-1)/a}+\mu_2$$

where μ_1 is the first Newtonian viscosity, μ_2 is the second Newtonian viscosity and $\dot{\gamma}$ is the shear rate. This equation represents a transition of η^* from μ_1 at low shear rates to μ_2 at high shear rates, and λ and a are the parameters characterizing the transition. Examples of the change in η^* with shear rate are illustrated in Fig.1.

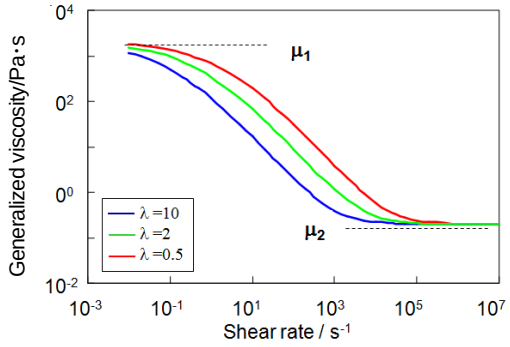

Fig.1 Change in the generalized viscosity with $\dot{\gamma}$

The generalized viscosity was determined for a grease prepared with synthetic hydrocarbon as the base oil and lithium stearate as the thickener (grease A in KYTB No.1) on a cone-on-plate rheometer giving shear in a sinusoidal angular oscillation manner. Results are shown in Fig.2 as a function of the shear rate and the oscillation frequency.

By using this generalized viscosity, a simplified EHL analysis has been made based on the 2-dimensional Ertel-Grubin theory. The dependence of μ_1 and μ_2 on pressure is assumed to be represented by two viscosity-pressure coefficients, α and β, such that $\mu_1 = \mu_{10}(1+\beta p)$ and $\mu_2 = \mu_{20}\exp(\alpha p)$, where μ_{10} and μ_{10} are the values of μ_1 and μ_2 at atmospheric pressure. Since the generalized viscosity depends on the oscillation frequency, certain "interpretation" has been necessary to use it in the EHL calculations.

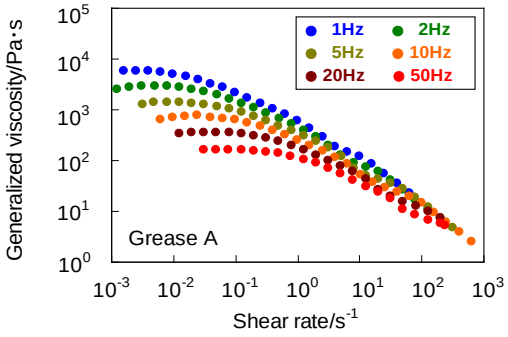

Fig.2 Generalized viscosity determined by rheometry

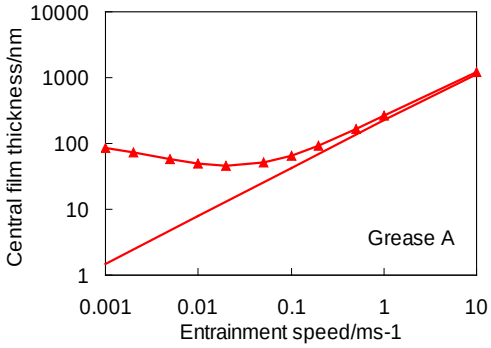

Fig.3 Film thickness calculated with η^*

The result is given in Fig.3. Though direct comparison with the experimental results of point contact is inadequate, Fig.3 shows that the film thickness follows the general EHL theory at high speeds, but at low speeds it deviates from the theory and increases again as speed is further reduced. This reproduces the peculiar behavior of grease observed in the optical interferometry.

Y. Kimura, T. Endo and D. Dong, "EHL with grease at low speeds", Jianbin Luo, Yonggang Meng, Tianmin Shao and Qian Zhao (eds.), Advanced Tribology - Proceedings of CIST2008 & ITS-IFToMM2008 Beijing, China (2009) pp.15-19.

KYODO YUSHI TECHNICAL BULLETIN

No.3 April 1, 2014

IN BALL BEARINGS, GREASE FORMS THICK ELASTOHYDRODYNAMIC LUBRICATION FILM AT LOW SPEEDS

Ultrathin-film optical interferometry revealed that, at extremely low speed, grease formed elastohydrodynamic(EHL) film which was much thicker than that with base oil alone. It was confirmed that that this characteristic behavior occurred in real ball bearings by electrical potential measurement.

Instead of the optical interferometry, electrical potential across the ball-race interfaces was measured. It keeps open-circuit potential in perfect EHL, but its time average lowers caused by occurrence of metal-to-metal contact. The potential was converted into the EHL film thickness with a master curve previously prepared by the relation between the measured potential in EHL with oil and the theoretical prediction by the Hamrock-Dowson theory.

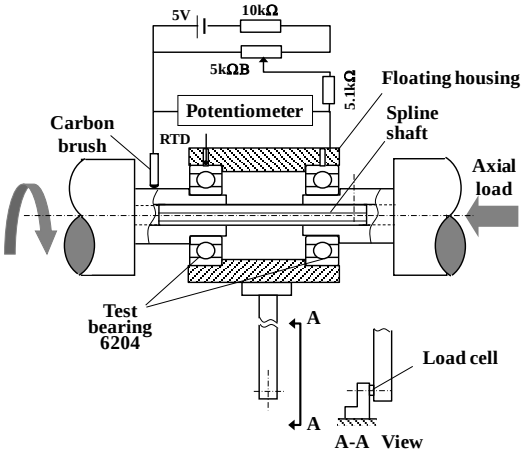

Fig.1 Experimental setup

As Fig.1 shows, two deep-groove ball bearings 6204 were mounted on each of the co-axial spindles connected by a splined shaft. Electrical potential was applied to the bearings in parallel, while in series to the ball-outer race and ball-inner race interfaces.

The sample grease, grease A was prepared with a synthetic hydrocarbon of viscosity 25mm^2/s, PAO4, as the base oil and lithium 12-hydroxy stearate as the thickener to have a consistency number 3.

At the high-speed range in Fig.2, the average potential with grease A ● was only slightly higher than that with PAO4 ○. Both ● and ○ lowered with the decrease of speed, but the lowering of ○ was more marked than that of ●. At the low-speed range below

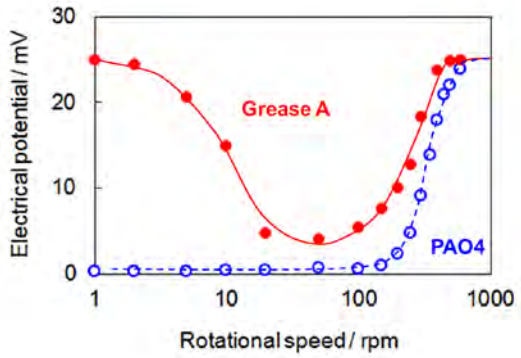

Fig.2 Change in electrical potential with speed

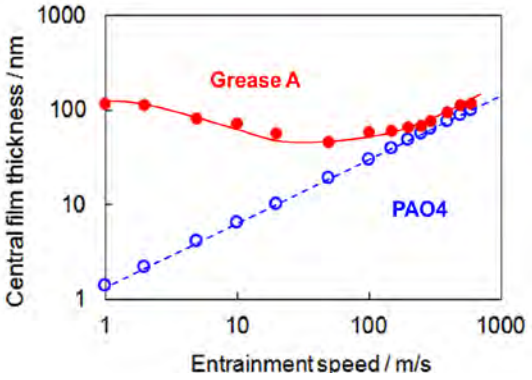

Fig.3 Change in central film thickness with speed

20rpm, while ○ remained almost nil, ● appreciably increased with further decrease in speed.

The average potential was converted into the central EHL film thickness, Fig.3, by using the master curve mentioned above. This result shows a common feature to that of the optical interferometry; that is, grease forms thick EHL film at low speeds caused by the increased viscosity at low shear rates.

D. Dong, T. Komoriya, T. Endo and Y. Kimura, "Formation of EHL film with grease in ball bearings at low speeds", J. JAST, vol.57, no.8 (2012) pp.568-574 (*in Japanese*).

KYODO YUSHI TECHNICAL BULLETIN

No.4 April 1, 2014

GREASE MARKEDLY REDUCES FRICTIONAL TORQUE OF BALL BEARINGS AT LOW SPEEDS

In the preceding issue it was reported that, at low speeds, grease formed elastohydrodynamic(EHL) film which was much thicker than that with base oil alone. In its consequence, grease markedly reduces frictional torque of the bearings at low speeds. Although its contribution to energy conservation seems limited, it will improve operability of devices.

The same setup was used as that for measuring EHL film thickness in ball bearings, Fig.1. A couple of deep-groove ball bearings 6204 were run under an axial load of 400N and rotational speed was changed. A bar extending from the floating housing pushed a load cell fixed on the frame to constrain the rotation of the housing and to monitor the frictional torque of the bearings.

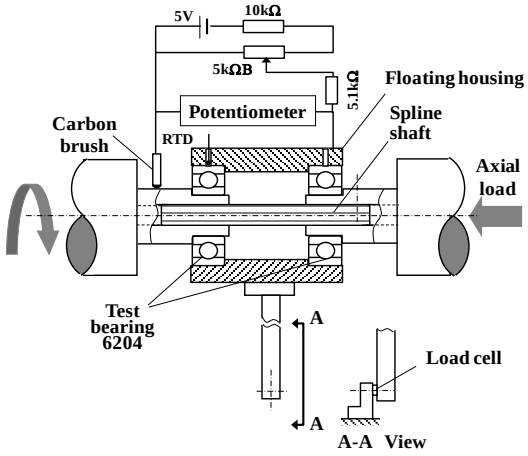

Fig.1 Experimental setup

Three sample greases A, B, C were prepared with synthetic hydrocarbon of different viscosity, A:25mm^2/s, B:81mm^2/s, C:741mm^2/s, as the base oils and lithium 12-hydroxystearate as the thickener; the concentration of the thickener was adjusted to have a consistency number 3. Experiments were made with each of the three sample greases and their base oils as lubricant.

Measured frictional torque is plotted in Figs.2 and 3 against the theoretical central EHL film thickness at the ball-race interfaces when lubricated with the base oil $h_{c,oil}$ after Hamrock and Dowson. Figure 2 shows that the three base oils exerted the same torque at high and medium speeds irrespective of their different viscosity, and it gradually decreased with decreasing speed. At low speeds when $h_{c,oil}$ was less than 40nm, the torque

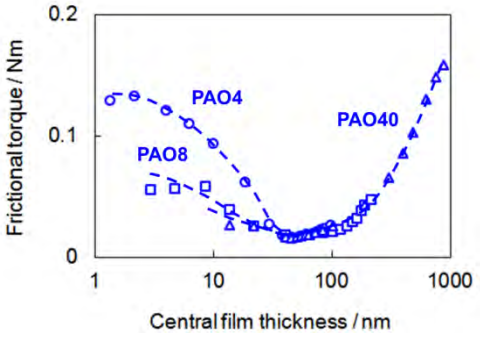

Fig.2 Change in frictional torque with $h_{c,oil}$: base oil

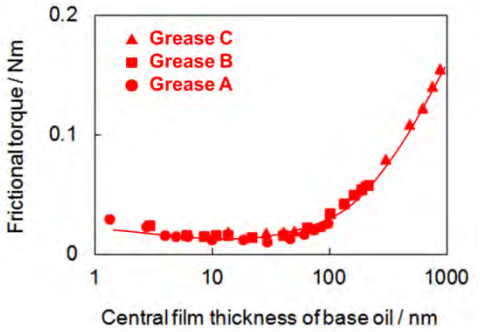

Fig.3 Change in frictional torque with $h_{c,oil}$: grease

increased with decreasing speed to different extents depending on their viscosity. When lubricated with grease, Fig.3, the change in the torque was similar to that with the base oil at high and medium speeds. At low speeds, however, the torque increased only slightly with decreasing speed, where the three sample greases showed practically the same torque being much smaller than that with base oil. Figure 2 for base oil represents the transition from EHL to mixed lubrication. In contrast, prevalence of EHL over the whole speed range characterizes the curve in Fig.3 for grease.

D. Dong, T. Komoriya, T. Endo and Y. Kimura, "Formation of EHL film with grease in ball bearings at low speeds", J. JAST, vol.57, no.8 (2012) pp.568-574 (*in Japanese*).

KYODO YUSHI TECHNICAL BULLETIN

No.5 February 1, 2015

FORMULATING IONIC LIQUID-BASED GREASE FOR SPACE MECHANISMS

Ionic liquids (IL) are salt composed of a cation and an anion and are liquid at room temperature. They have some beneficial features to lubricant for space mechanisms such as low volatility and stability over a wide temperature range. Further, some of them are superior to commonly used liquid lubricants for space in efficacy of additives to perfluoropolyethers (PFPE) and in better low temperature fluidity than multiply alkylated cyclopentane (MAC). By utilizing these features, an ionic liquid-based grease has been formulated aiming at the use for space mechanisms.

Selection of IL was performed in stages. First, 30 ILs were chosen out of more than 500 candidates for their non-toxicity, hydrophobicity and fluidity at -20°C. Secondly, 17 out of 30 ILs were chosen for their low volatility at high temperatures determined by themogravimetry/differential thermal analysis. In the third stage, low-temperature viscosity, surface tension and friction-and-wear characteristics in atmosphere were determined, and 7 ILs remained. With each of them, rust-preventing performance of several rust inhibitors against stainless steel was tested and, finally, a combination of an IL which had TFSA (bis[trifluoro-methylsulfonyl]amide) as the anion and a rust inhibitor which formed adsorbed film on steel surface was selected. Then several candidate greases were prepared with different thickeners and, after evaluating their consistency, bleeding and rust-preventing characteristics, a grease (IU) using aromatic polyurea as the thickener was formulated to have 60W penetration of 280.

Major properties of IU are compared with greases using PFPE and MAC as the base oil in Table 1. It shows that IU may operate at -40°C where only PFPE grease could be used.

Friction-and-wear properties of stainless steel SUS440C against itself in vacuum of 10^{-4}Pa were determined on a ball-on-disk machine lubricated with IU and the competitors under a maximum Hertzian pressure of 2.8GPa at sliding speed of 0.02m/s, Figs.1 and 2. IU displays low and stable friction and causes markedly low wear rate.

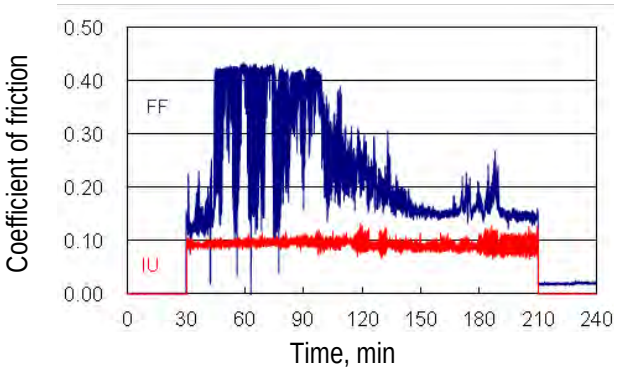

Fig.1 Coefficient of friction in vacuum

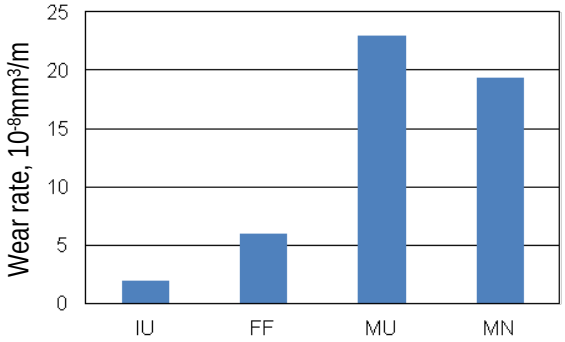

Fig.2 Wear rate in vacuum

Low volatility as well as low contamination by the evaporated constituents are required of the lubricants for space machinery. Total mass loss and collected volatile condensable materials were assessed, and it was confirmed that IU cleared the NASA criteria.

Table 1 Comparative properties of greases for space mechanisms

			IU	FF	MU	MN
Base oil	Type		IL	PFPE	MAC	
	Kinematic viscosity, mm²/s	40℃	20	144	104	
		–40℃	5000	5500	89000	
Thickener			Polyurea	PTFE	Polyurea	Na soap
Additives			Rust inhibitor	—	—	EP etc.
Penetration 60W			280	280	300	276

M. Hayama, "Research in application of ionic liquids to space lubricants", J. JAST, vol.58, no.12 (2013) pp.868-873 (*in Japanese*).

KYODO YUSHI TECHNICAL BULLETIN

No.6 January 11, 2016

REDUCATION IN FATIGUE LIFE IN HYDROGEN ENVIRONMENT

In rolling contact bearings used for automotive electrical components and auxiliary machineries, a reduction in fatigue life attributed to subsurface-initiated flaking resulting from white structure formation has been one of the critical issues. Considering that hydrogen has been noted as the cause, rolling contact fatigue tests were conducted in hydrogen and in air to study the differences in fatigue life and structural change with a focus on the effect of hydrogen permeation into steel.

Fig.1 shows the rolling four-ball tester used in this study. In the cup filled with lubricating oil, three freely-rolling bearing balls were set, on which another bearing ball was placed under static pressure to simulate flaking in rolling contact. The upper and lower balls were made of SUJ2 steel and had a diameter of 15.88 mm and 15.00 mm, respectively (in accordance with JIS B 1501). As summarized in Table 1, two different lubricating conditions, partial and full elastohydrodynamic lubrication (EHL) were achieved by changing load and the kinematic viscosity of test oil in air or in hydrogen. As for the tests in hydrogen, commercially available hydrogen was continuously supplied from the bottom of the cup.

Fig.2 shows the fatigue life, i.e., the number of contact before flaking occurred under different conditions. The life of the ball in hydrogen was significantly shorter than that in air regardless of test condition. Fig.3 shows the cross section of the tested upper ball, in which a white structure formed only in hydrogen. The white structure is considered to consist of an aggregate of ultrafine ferrite grains changed from a martensite structure and was observed in the vicinity of the maximum shear stress or shear stress amplitude areas. In hydrogen, it seems that repetitive contact between balls stimulated the formation of white structure accompanied by crack development leading to flaking at an early stage.

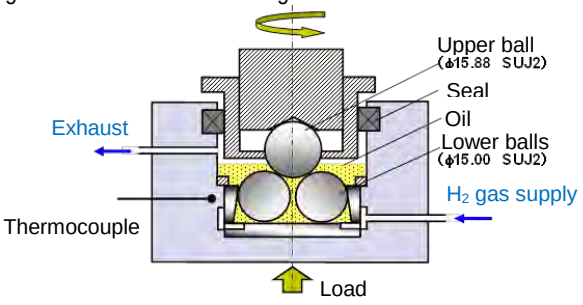

Fig.1 Main part of rolling four-ball tester

Table 1 Test condition

		Cond. 1	Cond. 2
Load, N (Max. Hertzian pressure, GPa)		2450(5.6)	980(4.1)
Lubricating oil		PAO400	PAO30
Kinematic viscosity, mm²/s	40℃	394	30.5
	100℃	40.1	5.9
Rotating speed/upper ball, rpm		1500	1500
Film thickness ratio		3<	1.4～2.0
Hydrogen gas supply, ml/min		15～20	15～20

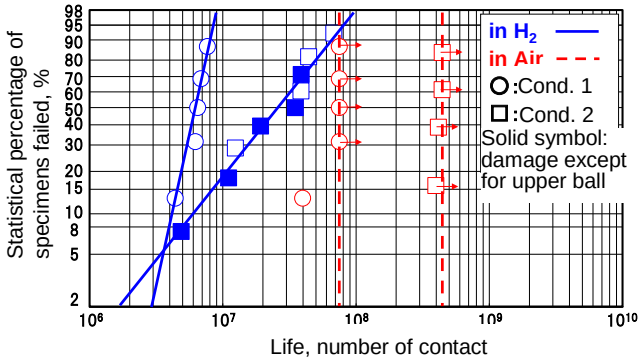

Fig.2 Fatigue life in hydrogen and in air

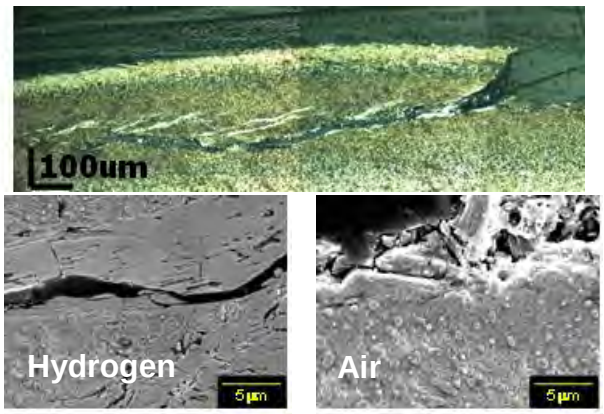

Fig.3 Cross-section of flaked upper ball

T. Endo, D. Dong, Y. Imai and Y. Yamamoto: Tribologist, 49, 10 (2004) 801.
Y.Imai, T.Endo and Y.Yamamoto: Proc. 63rd STLE Annual Meeting (2008) 346.

KYODO YUSHI TECHNICAL BULLETIN

No. 7 January 11, 2016

LUBRICANT'S CONTRIBUTION TO PREVENTION OF SHORTENED FATIGUE LIFE IN HYDROGEN

The rolling four-ball tests as reported in our previous issue (KYTB 6) demonstrated a reduction in fatigue life in hydrogen environment, where repetitive contact between balls stimulated the formation of white structure accompanied by crack propagation leading to flaking at an early stage. The same tests were carried out to examine the effect of lubricating oil additives on fatigue life in hydrogen and confirmed that certain types of rust inhibitors and anti-wear additives can prevent shortened fatigue life.

Fig.1 shows the rolling four-ball tester used in this study. In the cup filled with air or hydrogen, three bearing balls were rotated by another bearing ball placed on the top of them to simulate fatigue flaking in rolling contact. In our previous test (KYTB6), two PAOs of different kinematic viscosities were used as a lubricating oil to provide two lubrication regimes, full EHL (condition 1) and partial EHL (condition 2), where the ratio of minimum oil film thickness to composite surface roughness was above 3.0 and 1.4 to 2.0, respectively. The test results showed that a white structure formed only in hydrogen and the life of balls in hydrogen was shorter by one order of magnitude than that in air. With these results in mind, this study examined the effect of organometallic salts in lubricating oil on fatigue life in hydrogen.

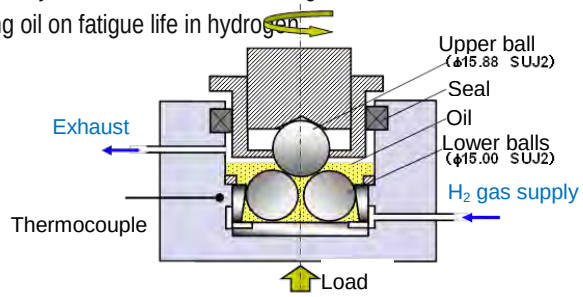

Fig.1 Main part of rolling four-ball tester

Table 1 shows the results of the tests under full EHL condition. Under this relatively mild lubrication condition, some organometallic salts used as a rust inhibitor or an anti-wear additive, especially organometallic salts A and B effectively extended the fatigue life when added alone. With organometallic salts A and B, no white structure formed likely because these rust inhibitors formed a dense adsorption film on the ball surface which prevented hydrogen from permeating into the steel.

Meanwhile, in the presence of solid contact under condition 2 (Table 2), a white structure formed even when organometallic salts A and B were added. Organometallic salt B had little effect in extending the fatigue life. The adsorption film seemed to have disappeared due to wear allowing hydrogen permeation. However, when used in combination with organometallic salt antiwear additives D or E, these rust inhibitors prevented white structure formation and significantly extended the flaking life. It is considered that the antiwear action of organometallic salts D and E helped the adsorption film remain and enabled extended life.

J. Imai and Y. Imai : Proceedings of the JAST Tribology Conference, Nagoya (2008-9) 351 (in Japanese).

Table 1 Results of rolling four-ball tests in hydrogen (Condition 1)

Additive	None	Rust inhibitor			Anti-wear additive	
		Organometallic salt A	Organometallic salt B	Organometallic salt C	Organometallic salt D	Organometallic salt E
L_{50} life, 10^6 rotations	6.4	75<	70<	22	75<	34
L_{10} life, 10^6 rotations	4.3	46	16	16	-	6.2
White structure formation	Yes	No	No	-	Yes	Yes

Table 2 Results of rolling four-ball tests in hydrogen (Condition 2)

Additive	None	Rust inhibitor		Rust inhibitor + Anti-wear additive		
		Organometallic salt A	Organometallic salt B	Organometallic salt A + D	Organometallic salt A + E	Organometallic salt B + E
L_{50} life, 10^6 rotations	33	112	32	230<	63	230<
L_{10} life, 10^6 rotations	9.6	69	20	-	24	-
White structure formation	Yes	Yes	Yes	No	Yes	No

KYODO YUSHI TECHNICAL BULLETIN

No.8 January 27, 2017

INVOLVEMENT OF HYDROGEN PERMEATION INTO STEEL IN SHORTENED FATIGUE LIFE

In our previous issues, KYTB 6 and 7, the rolling four-ball tests demonstrated that the fatigue life in hydrogen was associated with white structure formation and the life can be effectively extended by use of rust inhibitors and anti-wear additives. In this issue, back to the basics yet again, similar tests were conducted in deuterium to study how surrounding deuterium permeates into steel. Deuterium was detected in areas around cracks at levels of up to 70 to 110 times higher than natural hydrogen, indicating that it permeates into the cracked area of the steel surface to be concentrated.

Fig.1 show the rolling four-ball tester used in this study. In the cup filled with lubricating oil, three freely-rolling bearing balls were rotated by another bearing ball placed on the top of them to make an evaluation of fatigue life in rolling contact under static load. Unlike our previous tests in hydrogen H_2 (KYTB 6), the tests in this study were conducted in deuterium to draw a clear distinction from hydrogen present inherently in the steel ball. Deuterium is a hydrogen isotope and accounts for about 0.015% of all the naturally occurring hydrogen.

Similar to the previous tests in H_2, flaking occurred at the surface of the upper ball in a very short time and cracks were accompanied by white structure in their vicinity.

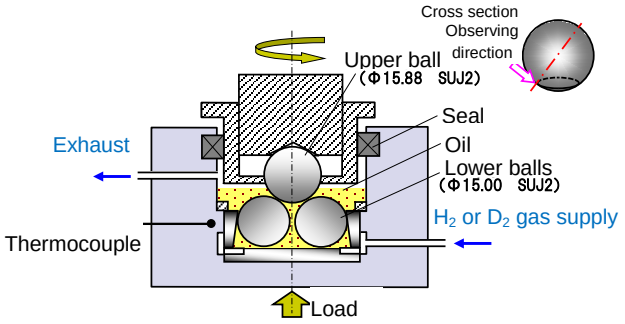

Fig.1 Main part of rolling four-ball tester

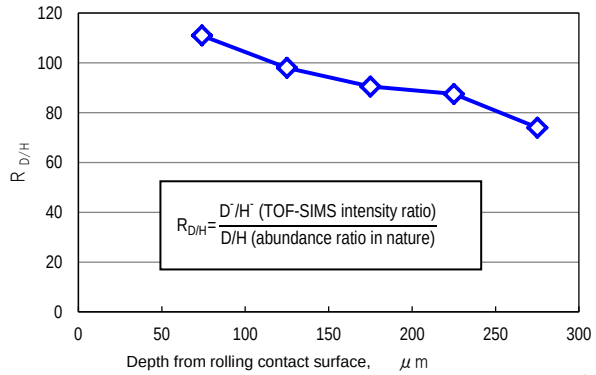

Fig.2 Deuterium abundance ratio for tested steel ball ($R_{D/H}$)

Okada, Nanao, Mori, Nakazawa, Ikejima, Muto, Endo, Imai, Aida: Proceedings of JAST Tribology Conference (Tokyo 2012-5) 277

TOF-SIMS analysis was carried out on the cross section as shown in the upper right in Fig.1 to study the existence and condition of hydrogen in tested steel ball. Fig.2 shows the difference in the abundance ratio, RD/H between deuterium in the steel ball and that in nature. Deuterium existed just beneath the ball surface at levels up to 70 to 100 times higher than hydrogen in nature but gradually reduced with depth to in the central part of the ball almost the same level as hydrogen in nature (1.6 times). Although deuterium in iron exhibited diffusion coefficients of about 0.7 to 0.9 times that of hydrogen, repetitive rolling contacts seemed to have induced scattering of hydrogen into the steel ball to produce a high-density subsurface layer.

Fig.3 (a) shows the cross section of flaked surface and Figs. 3 (b) and (c) show the chemical images of deuterium D- and deuterated iron FeD+ for the surface, respectively, which suggest higher levels of D- and FeD+ in the cracked area.

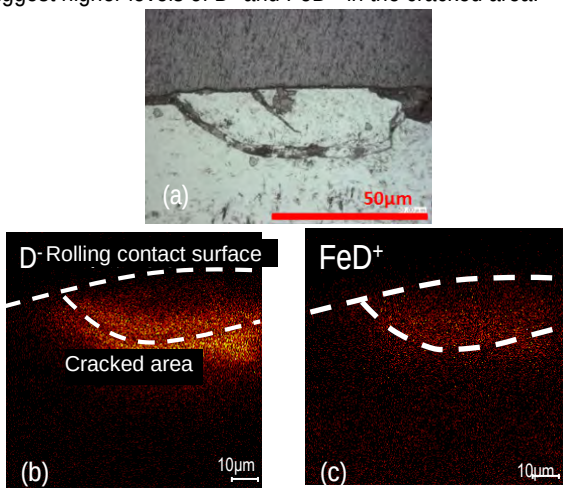

Fig.3 Chemical image of cracked area

KYODO YUSHI TECHNICAL BULLETIN

No. 9 January 27, 2017

NS compound's Contribution to Preventing Reduction of Fatigue Life in Hydrogen

It was reported in the last issue (KYTB 8) that the reduction of fatigue life in hydrogen is due to repeated rolling contact to allow hydrogen to permeate into steel to form a condensed layer beneath the steel surface. In this issue, following KYTB 7 where certain types of rust inhibitors and anti-wear additives effectively prevented hydrogen from permeating into steel, a nitrogen/sulfur compound (hereafter called NS compound) was examined to verify its potential for fatigue life extension.

Accelerated fatigue life testing was performed using a rolling four-ball tester as in KYTB 8 to evaluate the fatigue life under static load in hydrogen or in deuterium. In the test cup filled with lubricating oil, three freely-rolling bearing balls were rotated by another bearing ball placed on the top of them. In the experiment using the same four-ball tester reported in KYTB7, some organometallic salts effectively prevented flaking when added to the lubricating oils. To cope with today's severe operating conditions of rolling bearings for electric auxiliary components in vehicles, similar experiments were carried out to find a more effective additive for flaking prevention.

This experiment focused on the potential of a NS compound for fatigue life extension. Table 1 summarizes the results of four-ball life tests. Fig.1 shows the cross section of the rolling track of the upper ball tested with or without NS compound. While the ball lubricated with organometallic salt A, the most effective additive recognized in the previous experiment, had a L_{10} life of 46×10^6, NS compound prevented flaking up to a L_{10} life of 75×10^6 presenting no evidence of white structure formation.

Table 1 Additive's contribution to preventing the reduction of life

Additive	None	Organometallic salt A	NS compound
L_{50} life, 10^6	6.4	75<	75<
L_{10} life, 10^6	3.4	46	75<
White structure formation	Yes	No	No

Similar to KYTB 8, TOF-SIMS analysis was carried out on the cross section of the upper ball tested in deuterium to study the existence and condition of deuterium in steel. Fig.2 shows the chemical images of deuterium. The steel ball in the lubricating oil with NS compound had an abundance ratio of deuterium of nearly one as compared to that in nature, which represents that almost no deuterium permeated into steel. These results suggest that NS compound effectively prevents the reduction of fatigue life associated with hydrogen permeation into steel by forming a film on a rolling track surface.

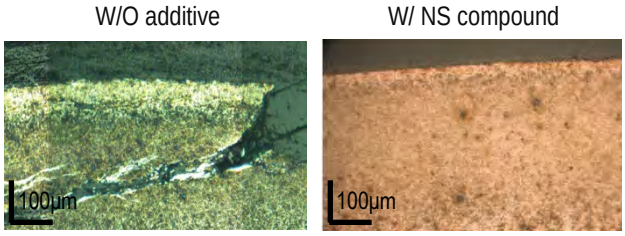

Fig.1 Cross-sectional observation

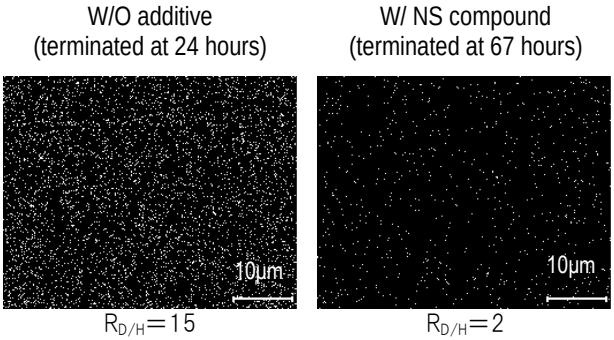

Fig.2 Chemical image of tested ball and deuterium ratio ($R_{D/H}$)

$$R_{D/H}=\frac{D^-/H^- \text{ (TOF-SIMS intensity ratio)}}{D/H \text{ (abundance ratio, in nature)}}$$

T. Komoriya, J. Imai, T. Endo, Y. Fukushima, M. Muto, S. Nakazawa, Y. Okada, H. Nanao and S. Mori: Proceedings of JAST Tribology Conference (Tokyo 2013-5) F13.

KYODO YUSHI TECHNICAL BULLETIN

No. 10 January 26, 2018

MEASUREMENT OF SOFT EHL FILM THICKNESS WITH GREASE

Engineering plastic materials like polyamide and polyacetal are widely used for worm wheels and other tribological elements under EHL conditions with grease. Low elastic modulus of those materials results in lower contact pressure than steel-to-steel contacts, and EHL of those contacts is called “soft EHL”.

An ultrathin-film optical interferometry system was used to measure the film thickness, where a steel ball was made contact with a transparent polycarbonate (PC) disk having similar elasticity to the engineering plastic materials. The ball and the disk were driven by respective motors to change entrainment speed from 0.1 to 1 m/s under a load of 10N at room temperature 25°C.

Four sample oils a to d are listed in Table 1. The viscosity-pressure coefficients were estimated by applying the H-D formula to the measured film thickness in the hard EHL experiments. Three sample greases A, B and C were made with the same base oil and different thickeners as shown in Table 2.

The central film thickness with sample oils is given in Fig.1 in the dimensionless parameters. All data fall on a straight line representing the H-D formula for soft EHL

$$H_c = 7.32U^{0.64}W^{-0.22}\{1-0.72\exp(-0.28k)\}$$

This implies that the film thickness in the present conditions has nothing to do with the piezo-viscous effect.

Figure 2 compares the central film thickness with the three sample greases and their base oil as a function of speed. With all sample greases, the film thickness is larger than that with their base oil alone and, although their base oil and consistency grade are the same, difference among the sample greases are found, the order being C>A>B, due to their different thickeners.

The curves in Fig.2 represent the predicted film thickness. This will be discussed based on separately measured rheological parameters of the sample greases.

Table 1 Sample oils

Sample oil	a PAO	b PAO	c *N-oil	d *P-oil
Viscosity @25°C, mPa·s	125	79.4	121	75.1
α @25°C, GPa^{-1}	15	14	26	20

*N-oil: naphthenic oil, P-oil: paraffinic oil

Table 2 Sample greases

Sample grease	A	B	C
Base oil Viscosity @25°C, mPa·s	PAO 49.5		
Thickener Concentration, mass%	Li-St 12	Li-OHSt 9.5	Urea 11
Penetration (60w)	296	297	294
Additive	None		

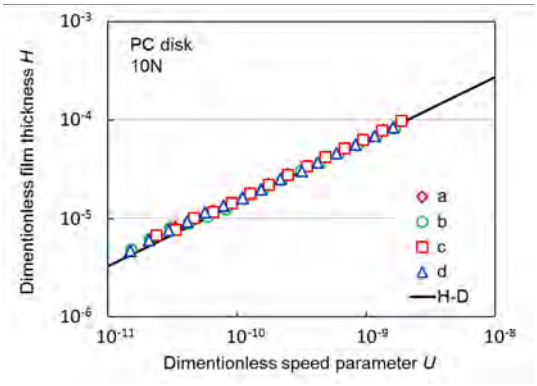

Fig.1 Dimensionless representation of central film thickness with different oils

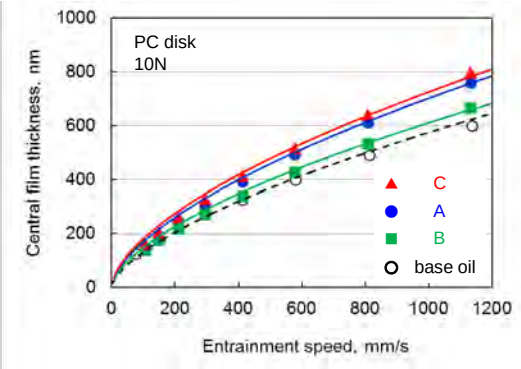

Fig.2 Film thickness with different greases

Kochi, Ichimura, Yoshihara, Dong and Kimura: Film thickness and Traction in Soft EHL with Grease, Tribology Online, 12, 4(2017), 171.

KYODO YUSHI TECHNICAL BULLETIN

No. 11 January 26, 2018

PREDICTION OF SOFT EHL FILM THICKNESS WITH GREASE

Soft EHL film thickness was measured by optical interferometry. The film thickness with greases is larger than that with their base oil alone and, difference among the sample greases are found due to their different thickeners. The possibility of prediction of the film thickness with grease is investigated on the basis of their rheology.

The apparent viscosity of the sample greases listed in table 1 was determined using a cone-on-plate rheometer. The cone was driven at stepwise increaseing shear rate from 100 to 40000s^{-1}. The results are plotted in Fig.1, in which the viscosity of the base oil is shown by the broken line. A rheology model after Bauer is employed:

$$\tau = \tau_y + k_1\dot{\gamma} + k_2\dot{\gamma}^n, \qquad \eta = \tau/\dot{\gamma} \tag{1}$$

where τ is the shear stress, $\dot{\gamma}$ is the shear rate, τ_y, k_1, k_2 and n are the rheological parameters. The viscosity of the base oil is reasonably used for the parameter k_1, and if the other rheological parameters are chosen to give the best fit, the curves in Fig. 1 agree with the experimental results with sufficient accuracy

At lower shear rates, the apparent viscosity decreases with increasing shear rate generally in a similar way, and the order of the apparent viscosity of the sample greases are B>C>A. However, the gradient of the curves are slightly different and, at high shear rates, the order changes into C>A>B.

The left side of rheological curves in Fig.1 shows the behavior of a plastic solid with a yield stress, and right side shows the behavior of Newtonian fluid, represented by the first and second terms in Eq.(1), and non-Newtonian behavior is by the third team, respectively.

Based on the rheological properties of greases, the prediction of the film thickness H_g in soft EHL contact is

Table 1 Sample greases

Sample grease	A	B	C
Base oil Viscosity @25ºC, mPa·s	PAO 49.5		
Thickener Concentration, mass%	Li-St 12	Li-OHSt 9.5	Urea 11
Penetration (60w)	296	297	294
Additive	None		

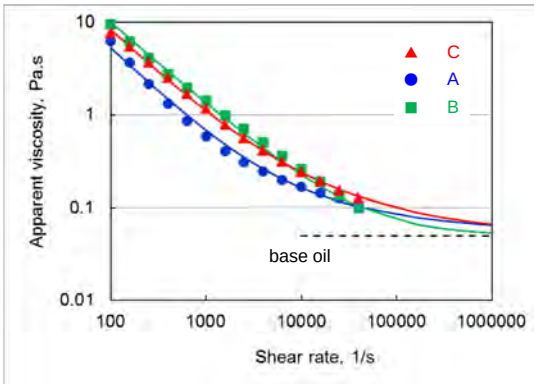

Fig.1 Apparent viscosity of sample greases

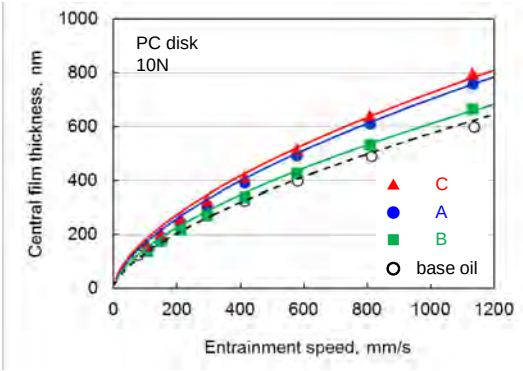

Fig.2 Film thickness with different grease

$$H_g / H_{oil} = \left(1 + m^n M\right)^{0.64} \tag{2}$$

where H_{oil} is the film thickness for base oil, M is the ratio of non-Newtonian effect to Newtonian effect, and m is a modifying coefficient changing from 1 to 1/n.

The curves in Fig.2 represent the central film thickness predicted with Eq.(2) for the sample greases. The prediction agrees well with the experimental results as a whole, though the predicted thicknesses are a little larger at lower speeds. The prediction procedure for hard EHL point contact is also proposed in present work.

Kochi, Ichimura, Yoshihara, Dong and Kimura: Film thickness and Traction in Soft EHL with Grease, Tribology Online, 12, 4(2017), 171.

KYODO YUSHI TECHNICAL BULLETIN
No. 12 January 22, 2019

TRACTION IN SOFT EHL CONTACT WITH GREASE

Reduction gears with a combination of a steel worm and an engineering plastic wheel are widely used. Their higher reliability and lower friction loss are required. In tribological terms, to reduce EHL traction is of current concern.

The traction between a steel ball and a PC disk was measured at a mean entrainment speed of 0.3 or 0.5m/s under a load of 20N at room temperature 25°C, and the slide-roll ratio changed from 0 to 50%.

Four sample oils a to d are listed in Table 1. Three sample greases A, B and C were made with the same base oil and different thickeners as shown in Table 2.

The traction in the soft EHL with three sample oils b, c and d is compared in Fig. 1, where difference in the traction coefficient with different type of oil is clearly observed showing the order c>d>b, in accordance with the order of the pressure-viscosity coefficient.

Figure 2 compares the traction with three sample greases and their base oil alone, at a mean entrainment speed of 0.5m/s. The traction coefficient with the greases is a little higher than that with their base oil, and the difference among the greases is insignificant.

The piezo-viscous effect must be taken into account. The reason is the traction is governed by the flow within a parallel region, under high pressure comparable to the Hertzian pressure. This suggests that theories on the traction proposed by Muraki and Kimura in the hard EHL

Table 1 Sample oils

Sample oil	a PAO	b PAO	c *N-oil	d *P-oil
Viscosity @25℃, mPa・s	125	79.4	121	75.1
α @25℃, GPa^{-1}	15	14	26	20

*N-oil: naphthenic oil, P-oil: paraffinic oil

Table 2 Sample greases

Sample grease	A	B	C
Base oil Viscosity @25℃, mPa·s	PAO 49.5		
Thickener Concentration, mass%	Li-St 12	Li-OHSt 9.5	Urea 11
Penetration (60w)	296	297	294
Additive	None		

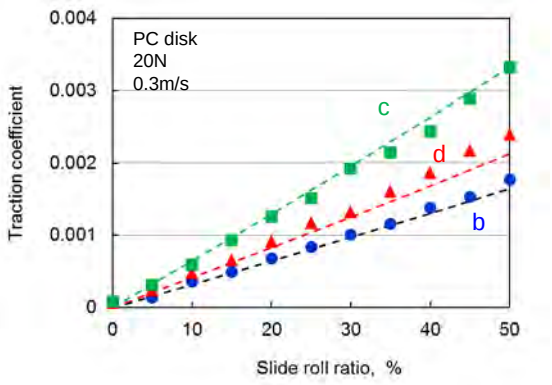

Fig.1 Traction coefficient with different oils

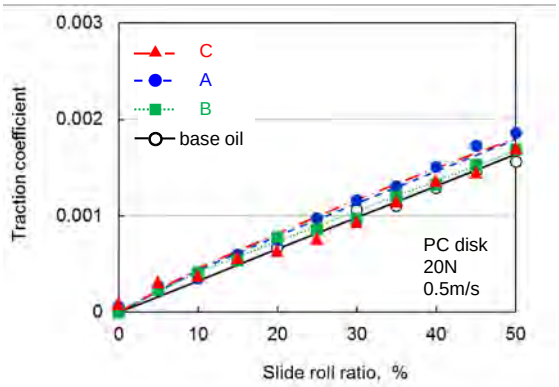

Fig.2 Traction coefficient with different greases

can be used in the present case. For the linear viscous and isothermal region, the traction coefficient μ is further simplified to give

$$\mu = \eta_0 \exp(\alpha P_{mean}) \times \Delta u / h_c \times 1/ P_{mean}$$

where η_0 is the apparent viscosity, α is the viscosity-pressure coefficient, P_{mean} is the mean Hertzian pressure, and Δu is the speed difference between the ball and the disk. The central film thickness h_c is given by previous issue (KYTB 11). The predicted results are shown in the Figs.1 & 2 as corves, and reasonable agreement with the experimental results.

Kochi, Ichimura, Yoshihara, Dong and Kimura: Film thickness and Traction in Soft EHL with Grease, Tribology Online, 12, 4(2017), 171.

KYODO YUSHI TECHNICAL BULLETIN

No. 13 February 22, 2019

OBSERVATION OF THICKENER STRUTURE IN GREASE

Lubricating grease is defined as “a solid-to-semi fluid product of dispersion of a thickening agent in a liquid lubricant”. Although it is important to know the thickener state of being in grease, thickener structure in grease still remains to be explained. The observation has traditionally been made using an electron microscope, TEM or SEM. However, it requires grease sample processing such as dilution, dispersion and oil extraction. This study aims to make direct observations of thickener structure in grease using a confocal laser fluorescence microscope, CLFM.

A CLFM is capable of noninvasively observing a specimen to generate a distinct in-focus image at high resolution by taking advantage of both confocal optical system which can selectively detect fluorescent light coming from the focused point of a specimen and fluorescent microscopy which measures fluorescent light when the specimen illuminated with excitation light moves from excited state to normal state. In this study, a laser beam emitting a wavelength of 488nm was employed as excitation light. Sampling in a X-Y direction and shifting in a Z direction were performed at intervals of 0.4μm and 0.5μm, respectively.

Grease sample was prepared with diurea as the thickener and mineral oil as the base oil and had a thickener content of 4mass%. The grease sample of 10-20mg was placed on a glass slide and gently pressed with a cover glass to achieve a thickness of 20-30μm.

Fig. 1 shows a 3-D image of sample grease, where worm-like fibers are present to form a network structure.

To further examine the fibers shown in Fig. 1, the grease sample was diluted 20 times with its base oil. The 3-D image obtained for diluted grease shows that there are fibers of a few μm in diameter and 10-50μm in length coupled with finer fibers (Fig. 2).

The SEM image of grease, Fig. 3, indicated that fine thickener fibers of <1μm in diameter and a few μm in length are present, being bundled together to form thick fibers of 2-3μm in diameter and 40μm in length. These thick fibers of the same size as those in the CLFM images provide sufficient evidence to consider that the 3-D images show the thickener network structure in grease.

M.Yoshihara & T. Moriuchi: NLGI Spokesman, 81, 1 (2017), 28.

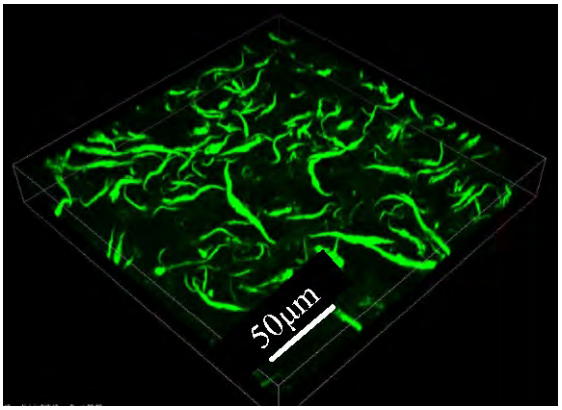

Fig.2 3-D structure of diluted grease

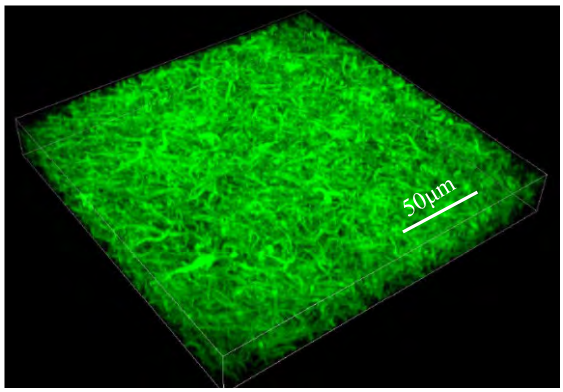

Fig.1 3-D structure of sample grease

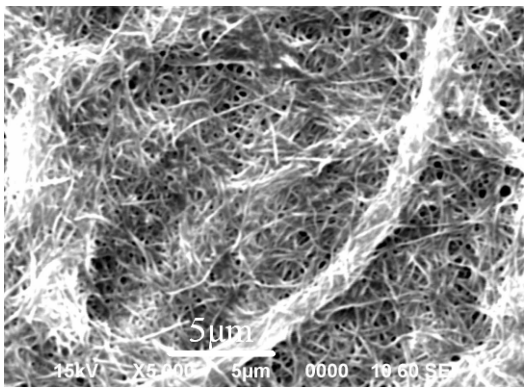

Fig.3 SEM image of sample grease

KYODO YUSHI TECHNICAL BULLETIN

No. 14 April 16, 2021

DECOMPOSITION OF OILS BY ACTION OF DISCHARGE PLASMA(1)

-ORIGINAL DISCHARGE PLASMA GENERATOR-

One of the main problems in alternators is the extremely short fatigue life of the rolling bearings. As a possible cause of the short life, it has been assumed that hydrogen is produced inside the bearing and then it penetrates into the bearing material to cause hydrogen embrittlement, which results in the short life. However, it is unknown from where the hydrogen comes. On the other hand, it is reported that plasma is generated in oil lubrication. In this study, we invented a new apparatus that generates discharge plasmas in oil. Using it, we have investigated whether hydrogen is produced or not through oil decomposition by discharge plasma action.

Figure 1 (a) and (b) shows the principle of the needle-plate electrodes type plasma generator that we invented and the chromatograph to analyze the gases evolved by decomposition of oils due to discharge plasma action, respectively. Discharge was geneared between the needle and plate electrodes in oil, where a voltage was applied between the electrodes using an external high voltage power supply (HV). Prior to the experiments, the chamber was filled with dry air by passing dry air into the chamber for 30 seconds to eliminate the effect of moisture. The discharging was generated for 10 seconds, during which current and voltage were monitored using an oscilloscope. After discharging, leaving it for 20 seconds, the gases produced in the chamber were sampled using a microsyringe and then they were inserted into the chromatographic column to measure the amount of H_2.

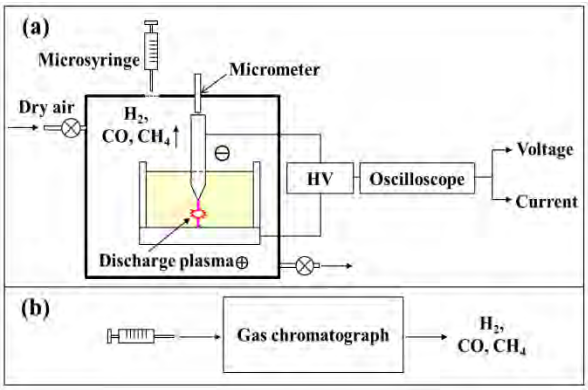

Fig.1 Schematic view of discharge plasma generator.

Figure 2 shows the relation between the amount of hydrogen produced in *n*-hexadecane for 10 seconds discharging and the electrodes distance. It is shown that the amount of hydrogen decreases with increasing electrodes distance, having the smallest data variation at 50μm. Figure 3 shows the amount of hydrogen versus discharge time at the electrodes distance of 50μm in *n*-hexadecane. The amount of hydrogen rapidly increases with increasing discharge time and then saturates at 30 to 40 s. Based on these data, we adopted the electrodes distance of 50μm and the discharge time of 30 s for the experimental condition, in which we could successfully acquire reproducible data.

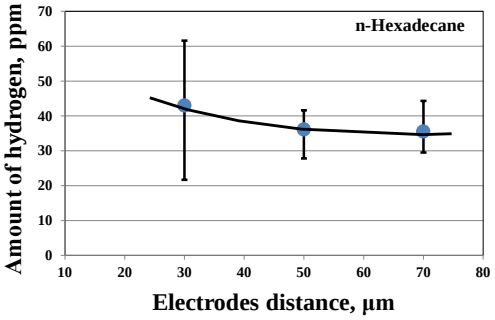

Fig.2 Dependence of hydrogen production on electrodes distance

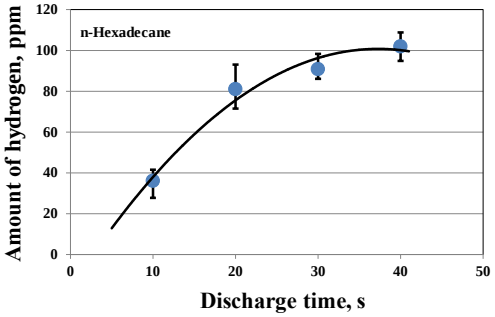

Fig.3 Dependence of hydrogen production on discharge time

The needle-plate electrodes discharge plasma generator invented in this study enabled discharge plasma generation, not only in air but also in oil. Using the plasma generator, we have verified that the straight-chain hydrocarbon oil is decomposed by discharging in oil to produce hydrogen. Reaction mechanisms of oil decomposition due to plasma action will be further examined from various perspectives for both in base oils and additives to develop new applied plasma technologies.

IIJIMA, M., NAKAYAMA, K.: JAST Tribology Conference, 2017 Tokyo, C13
NOYAMA, S., NAKAYAMA, K. et al.: JAST Tribology Conference, 2017 Takamatsu, A20

KYODO YUSHI TECHNICAL BULLETIN

No. 15 April 16, 2021

DECOMPOSITION OF OILS BY ACTION OF DISCHARGE PLASMA (2)
-HYDROCARBON COMPOUNDS-

In our last issue, a needle-plate electrodes discharge plasma generator was constructed. Using it, various hydrocarbon compounds were tested, and we found that they are decomposed by discharge plasma action to produce hydrogen. This report summarizes our findings of how hydrogen production is affected by the structure of aliphatic/aromatic hydrocarbon compounds.

Table 1 shows the oil species, molecular and structural formulae and hydrogen productions caused by discharge plasma action on the hydrocarbon compounds, where the amount of hydrogen production indicates the percentage when that of *n*-hexadecane is 100. Aliphatic hydrocabons show little difference in the volume of hydrogen productions, which range from 91 to 106 %. However over all types of aliphatic, straight, blanched and cyclic compounds tested, the hydrogen production volume increases with increasing molecular weight, i.e., with increasing molecular chain length.

Table 1 Hydrocarbon compound samples – molecular structure and hydrogen production

Oil species		Molecular formula	Structural formula	H_2, %
Aliphatics (Straight)	*n*-Dodecane	$C_{12}H_{26}$	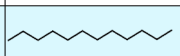	90
	n-Tetradecane	$C_{14}H_{30}$	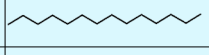	96
	n-Hexadecane	$C_{16}H_{34}$	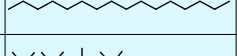	100
Aliphatics (Blanched)	2,2,4,4,6,8,8-Heptamethyl nonane	$C_{16}H_{34}$	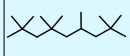	97
	2,6,10,14-Tetramethyl pentadecane	$C_{19}H_{40}$	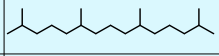	104
	2,6,10,15,19,23-Hexamethyl tetracosane (Squalane)	$C_{30}H_{62}$	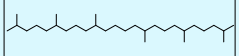	106
Aliphatics (Cyclic)	Bicyclohexyl	$C_{12}H_{22}$		98
	n-Octyl cyclohexane	$C_{14}H_{28}$	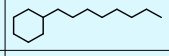	102
	n-Dodecyl cyclohexane	$C_{18}H_{36}$	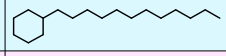	104
Aromatics (Mono-)	*n*-Octyl benzene	$C_{12}H_{22}$	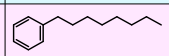	94
	n-Dodecyl benzene	$C_{14}H_{28}$	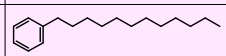	93
Aromatics (Di-)	Diphenylmethane	$C_{13}H_{12}$	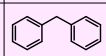	2
	Diphenylpropane	$C_{15}H_{16}$	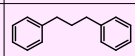	3
	Cis-1,2-Diphenylethylene	$C_{14}H_{14}$	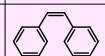	2
	4-Methyl-2,4-Diphenyl-1-Pentene	$C_{18}H_{28}$	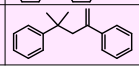	72

As for aromatic hydrocarbon compounds, aromatics having one benzene ring with a linear aliphatic chain containing 8 or more carbon numbers produce hydrogen at almost the same level as that of aliphatic hydrocarbon compounds, but those having two benzene rings with aliphatic hydrocarbon groups between them produce less hydrogen. Prticularly, hydrogen production is extremely low for aromatics having 1 to 3 methylene groups (-CH_2-) and a methine group (-CH=) between the rings.

Figure 1 shows the amount of hydrogen as a function of, $\%C_A$, the ratio of the number of carbon atoms in an aromatic ring to all carbon atoms in the molecule. In aromatic hydrocarbon compounds, the amount of hydrogen production significantly depends on their molecular structure, and the hydrogen production decreases with increasing $\%C_A$, to be minimized at and above 80% .

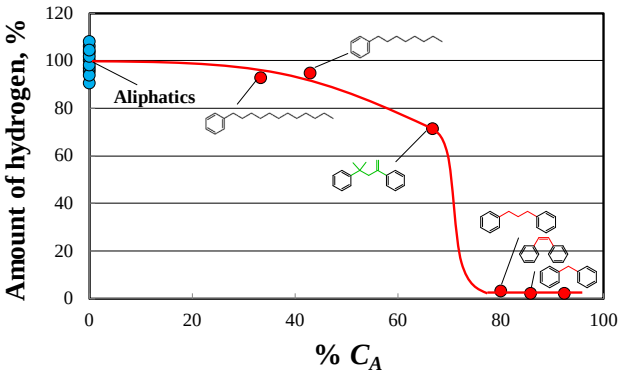

Fig. 1 Dependence of hydrogen production on $\%C_A$

These results suggest that aromatic oils can be a promising lubricating oil to be developed for avoiding the shortened service life of rolling bearing through white structure flaking.

NOYAMA, S., IIJIMA, M., DONG, D., NAKAYAMA, K.: JAST Tribology Conference, 2018 Spring Tokyo, E4

KYODO YUSHI TECHNICAL BULLETIN

No. 16 April 16, 2021

DECOMPOSITION OF OILS BY ACTION OF DISCHARGE PLASMA (3)
-OXYGEN CONTAINING HYDROCARBON COMPOUNDS-

In the last issue, various hydrocarbon compounds were tested using a newly invented needle-plate electrodes discharge plasma generator and we found that they were decomposed by discharge plasma action to produce hydrogen. This report summarizes our findings of how hydrogen production is affected by the structure of oxygenated hydrocarbon compounds.

Table 1 shows the oil species, structural formula, hydrogen production caused by discharge plasma action and volume resistivity of the oxygenated hydrocarbon compounds tested, where the amount of hydrogen production indicates the percentage when that of *n*-hexadecane is 100. In the ester compounds, the volume resistivity and hydrogen production volume is increased with increasing in the alkyl chain length. This trend does not depend on the posiotion of the alkyl chain, neither at the center or at the ends. On the other hand, in the ether compounds, the volume resistivity and the amount of hydrogen are decreased with increasing in the number of oxygen atoms in the molecule. Glycol compounds showed lower volume resistivity than other oxygenated hydrocarbon compounds and no hydrogen production.

Table 1 Oxygenated hydrocarbon compound samples – molecular structure, hydrogen production and volume resistivity

Oil Species		Structural formula	H_2, %	Volume resistivity Ω・cm
Di-Ester	Dimethyl Malonate	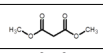	0	2.2×10^{7}
	Dibutyl Malonate	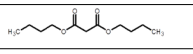	0	4.1×10^{8}
	Dihexyl Malonate	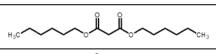	1	4.4×10^{9}
	Dimethyl Succinate	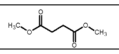	0	2.7×10^{7}
	Dimethyl Glutarate	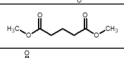	0	6.0×10^{7}
	Dimethyl Adipate	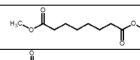	0	1.1×10^{9}
	Dimethyl Sebacate	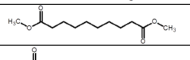	17	3.5×10^{9}
	Diethyl Sebacate	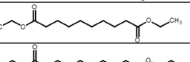	67	1.3×10^{10}
	Dibutyl Sebacate	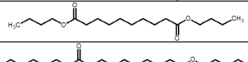	93	6.1×10^{10}
	Dihexyl Sebacate	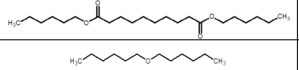	95	2.2×10^{11}
Ether	Dihexyl Ether	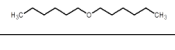	103	6.3×10^{12}
	Dioctyl Ether	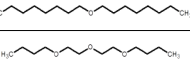	91	2.2×10^{13}
Glycol Ether	Diethylene Glycol Dibutyl Ether	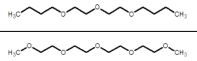	88	1.4×10^{10}
	Tetraethylene Glycol Dimethyl Ether	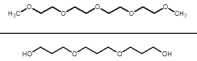	0	3.5×10^{7}
Glycol	Tripropylene Glycol	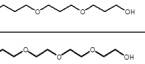	0	2.0×10^{7}
	Tetraethylene Glycol	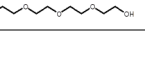	0	6.8×10^{6}

Figure 1 shows the amount of evolved hydrogen as a function of volume resistivity of the ester, ether and glycol compounds tested. No hydrogen is produced at and below the volume resistivity of 1.1×10^{9} Ω・cm. However at and above 3.5×10^{9} Ω・cm, hydrogen is clearly produced, the volume of which increases steeply with the volume resistivity, approaching to an almost constant maximum value. This means that there exists a critical volume resistivity to cause hydrogen production, which is 10^{9}Ω・cm. It should be noted that for all types of oxygenated hydrocarbon compound tested, the relation between hydrogen production and volume resistivity lies on a single curved line.

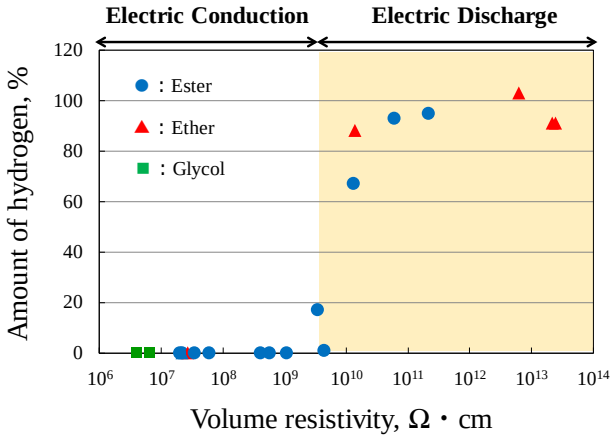

Fig. 1 Dependence of hydrogen production on volume resistivity

These results suggest that oils having volume resistivity of less than 10^{9} Ω・cm can be a promising lubricating oil to be developed for avoiding the shortened (fatigue) service life of rolling bearing through white structure flaking.

Noyama, S., Iijima, M., Dong, D., Nakayama, K.: JAST Tribology Conference, 2018 Autumn Ise, A34
Noyama, S., Iijima, M., Dong, D., Nakayama, K.: JAST Tribology Conference, 2019 Spring Tokyo, A2